Forward sensitivity analysis of the index-3 augmented Lagrangian formulation with projections

Daniel Dopico[1], Francisco González[1], Alberto Luaces[1], Mariano Saura[2], Daniel García-Vallejo[3]

[1] Laboratorio de Ingeniería Mecánica,
University of A Coruña.
Mendizábal s/n, 15403. Ferrol, Spain.
{ddopico, f.gonzalez, aluaces}@udc.es

[2] Dpto. de Ingeniería Mecánica,
Universidad Politécnica de Cartagena.
C/ Dr. Fleming s/n, 30202. Cartagena, Spain.
msaura.sanchez@upct.es

[3] Dpto. de Ingeniería Mecánica y Fabricación,
Universidad de Sevilla.
Camino de los Descubrimientos, s/n, 41092. Sevilla, Spain.
dgvallejo@us.es

Abstract

Optimizing the dynamic response of mechanical systems is often a necessary step during the early stages of product development cycles. For gradient-based optimization methods, this is a complex problem that requires to carry out the sensitivity analysis of the system dynamics equations. These are often expressed as a highly nonlinear system of Ordinary Differential Equations (ODEs) or Differential Algebraic Equations (DAEs), if a dependent set of generalized coordinates with its corresponding kinematic constraints is used to describe the motion. Two main techniques are currently available to perform the sensitivity analysis of a multibody system, namely the direct differentation and the adjoint variable methods.

In this paper, we derive the equations that correspond to the direct sensitivity analysis of the index-3 augmented Lagrangian formulation with velocity and acceleration projections (ALI3-P formulation). The analysis is limited to systems with holonomic constraints. The evaluation of the system sensitivities requires the solution of three Tangent Linear Models (TLMs): the first one, which is an index-3 augmented Lagrangian DAE problem, corresponds to the dynamics equations of motion, and the two additional ones are for the velocity and acceleration projections, which are nonlinear systems of equations. The method was validated in the sensitivity analysis of a five-bar linkage with spring elements, which had been used as benchmark problem for similar multibody dynamics formulations.

Keywords: multibody system dynamics, sensitivity analysis, index-3 augmented Lagrangian formulation

1. Introduction

Sensitivity analysis of the dynamics of multibody systems is essential for design optimization and optimal control. Dynamic sensitivities, when needed, are often calculated by means of finite differences but, depending on the number of parameters involved, this procedure can be very demanding in terms of time, and the accuracy obtained can be very poor in many cases.

In previous works, the sensitivity equations of index-3 DAE, index-1 DAE, Baumgarte, and penalty formulations [1, 2, 3, 4, 5, 6, 7, 8] were derived, using either direct differentiation (forward sensitivity), adjoint variable (adjoint sensitivity) or both methods depending on the publication.

The index-3 augmented Lagrangian formulation with velocity and acceleration projections (the ALI3-P formulation) is an efficient and robust method to carry out the forward-dynamics simulation of multibody systems modeled in dependent coordinates, which outperforms the behavior of the aforementioned formulations in many cases. It was extensively used for the real-time simulation of different systems with human and hardware in the loop, some of them including complex phenomena like flexibility [9], contact with friction [10, 11], non-holonomic constraints [12], and singular configurations [13].

In [14] the sensitivity analysis equations of several formulations of interest for this work were derived. Based on those previous derivations, the forward sensitivity equations of the ALI3-P formulation presented in [12] are derived here and applied to a test case.

2. ALI3-P formulation

The equations of motion of the ALI3-P formulation were thoroughly described in [12] for holonomic and non-holonomic systems. A summary of the basics of the formulation is provided here; in this work a simplified version of the formulation, with holonomic constraints only and without the generalized-α integration scheme, will be used.

Let us consider a multibody system modeled in terms of a set of parameters, $\boldsymbol{\rho} \in \mathbb{R}^p$, with $\mathbf{q}(\boldsymbol{\rho},t) \in \mathbb{R}^{n_c}$ dependent coordinates related by m holonomic constraints $\boldsymbol{\Phi}(\mathbf{q},\boldsymbol{\rho},t) \in \mathbb{R}^m$. The formulation equations of motion (EOM) have the following expressions

$$\mathbf{M}\ddot{\mathbf{q}} + \boldsymbol{\Phi}_{\mathbf{q}}^{\mathrm{T}}\left(\boldsymbol{\lambda}^{*(i+1)} + \boldsymbol{\alpha}\boldsymbol{\Phi}\right) = \mathbf{Q} \tag{1a}$$

$$\boldsymbol{\lambda}^{*(i+1)} = \boldsymbol{\lambda}^{*(i)} + \boldsymbol{\alpha}\boldsymbol{\Phi}^{(i+1)};\, i > 0 \tag{1b}$$

where $\mathbf{M}(\mathbf{q},\boldsymbol{\rho}) \in \mathbb{R}^{n_c \times n_c}$ is the mass matrix of the system, $\boldsymbol{\Phi}_{\mathbf{q}}(\mathbf{q},\boldsymbol{\rho},t) \in \mathbb{R}^{m \times n_c}$ is the Jacobian matrix of the vector of constraints, $\boldsymbol{\alpha} \in \mathbb{R}^{m \times m}$ is a diagonal matrix containing the penalty factors associated with the constraints, $\mathbf{Q}(\mathbf{q},\dot{\mathbf{q}},\boldsymbol{\rho},t) \in \mathbb{R}^{n_c}$ is the vector of generalized forces, $i = 0,1,2,...$ is the iteration index of the approximate Lagrange multipliers $\boldsymbol{\lambda}^*(\boldsymbol{\rho},t) \in \mathbb{R}^m$. These converge for $i \to \infty$ to $\boldsymbol{\lambda}$, which are the ones resulting from the solution of the classical index-3 DAE system.

The algorithm in Eqs. (1) is often combined with a numerical integration scheme to solve the dynamics equations following a Newton-Raphson iterative approach. Several formulas can be used; the Newmark method [15] is a popular choice

$$\dot{\mathbf{q}}_n = \frac{\gamma}{\beta h}\mathbf{q}_n - \hat{\dot{\mathbf{q}}}_{n-1}; \qquad \text{where} \;\; \hat{\dot{\mathbf{q}}}_{n-1} = \frac{\gamma}{\beta h}\mathbf{q}_{n-1} + \left(\frac{\gamma}{\beta} - 1\right)\dot{\mathbf{q}}_{n-1} + h\left(\frac{\gamma}{2\beta} - 1\right)\ddot{\mathbf{q}}_{n-1} \tag{2a}$$

$$\ddot{\mathbf{q}}_n = \frac{1}{\beta h^2}\mathbf{q}_n - \hat{\ddot{\mathbf{q}}}_{n-1}; \qquad \text{where} \;\; \hat{\ddot{\mathbf{q}}}_{n-1} = \frac{1}{\beta h^2}\mathbf{q}_{n-1} + \frac{1}{\beta h}\dot{\mathbf{q}}_{n-1} + \left(\frac{1}{2\beta} - 1\right)\ddot{\mathbf{q}}_{n-1} \tag{2b}$$

where β and γ are scalar parameters of the integrator, and h is the integration step-size. Subscript n denotes the time step. If $\beta = 0.25$ and $\gamma = 0.5$, Eqs. (2) are those of the well-known trapezoidal rule. When the expressions in Eqs. (2) are introduced in the equations of motion (1a), establishing the dynamic equilibrium at time t_n, the system dynamics is formulated as the following system of nonlinear equations

$$\mathbf{g}(\mathbf{q},\dot{\mathbf{q}},\boldsymbol{\rho}) = \left[\mathbf{M}\mathbf{q} + \beta h^2\boldsymbol{\Phi}_{\mathbf{q}}^{\mathrm{T}}\left(\boldsymbol{\lambda}^{*(i+1)} + \boldsymbol{\alpha}\boldsymbol{\Phi}\right) - \beta h^2\mathbf{Q}\right]_n - \beta h^2\mathbf{M}\hat{\ddot{\mathbf{q}}}_{n-1} = \mathbf{0} \tag{3}$$

In each iteration of the Newton-Raphson process an increment of the generalized coordinates is evaluated

$$\left[\frac{\mathrm{d}\mathbf{g}(\mathbf{q})}{\mathrm{d}\mathbf{q}}\right]^i \Delta\mathbf{q}^{i+1} = -\left[\mathbf{g}(\mathbf{q})\right]^i \tag{4}$$

with the approximate tangent matrix

$$\left[\frac{\mathrm{d}\mathbf{g}(\mathbf{q})}{\mathrm{d}\mathbf{q}}\right] = \mathbf{M} + \gamma h\mathbf{C} + \beta h^2\left(\boldsymbol{\Phi}_{\mathbf{q}}^{\mathrm{T}}\boldsymbol{\alpha}\boldsymbol{\Phi}_{\mathbf{q}} + \mathbf{K}\right) \tag{5}$$

where $\mathbf{K} = -\mathbf{Q}_{\mathbf{q}} = -\partial\mathbf{Q}/\partial\mathbf{q}$ and $\mathbf{C} = -\mathbf{Q}_{\dot{\mathbf{q}}} = -\partial\mathbf{Q}/\partial\dot{\mathbf{q}}$. The Lagrange multipliers $\boldsymbol{\lambda}^*$ can also be updated during this iterative process with the expression in Eq. (1b). Upon convergence of the iterative process at time-step t_n, the sets of positions, $\mathbf{q}_n$, velocities, $\dot{\mathbf{q}}_n^*$ and accelerations $\ddot{\mathbf{q}}_n^*$, are obtained. The set of positions $\mathbf{q}$ exactly fulfills the constraint equations $\boldsymbol{\Phi} = \mathbf{0}$, within the convergence tolerance of the algorithm; on the contrary, the satisfaction of $\dot{\boldsymbol{\Phi}} = \mathbf{0}$ and $\ddot{\boldsymbol{\Phi}} = \mathbf{0}$ is not as good and the sets of velocities and accelerations, $\dot{\mathbf{q}}_n^*$ and $\ddot{\mathbf{q}}_n^*$ have to be projected onto their corresponding manifolds to obtain their clean counterparts, $\dot{\mathbf{q}}_n$ and $\ddot{\mathbf{q}}_n$. The expression for velocities is,

$$\left(\mathbf{P} + \varsigma\boldsymbol{\Phi}_{\mathbf{q}}^{\mathrm{T}}\boldsymbol{\alpha}\boldsymbol{\Phi}_{\mathbf{q}}\right)\dot{\mathbf{q}}^{(i+1)} = \mathbf{P}\dot{\mathbf{q}}^* - \boldsymbol{\Phi}_{\mathbf{q}}^{\mathrm{T}}\left(\boldsymbol{\sigma}^{(i+1)} + \varsigma\boldsymbol{\alpha}\boldsymbol{\Phi}_t\right) \tag{6a}$$

$$\boldsymbol{\sigma}^{(i+1)} = \boldsymbol{\sigma}^{(i)} + \varsigma\boldsymbol{\alpha}\dot{\boldsymbol{\Phi}} \tag{6b}$$

where $\boldsymbol{\sigma}$ are the Lagrange multipliers associated to the projections of velocities, $\mathbf{P}$ is the weight matrix (or projection matrix) and ς is a scalar constant for the weighting of the constraints in the projection.

Similar equations hold for the projections of accelerations.

$$\left(\mathbf{P} + \varsigma\boldsymbol{\Phi}_{\mathbf{q}}^{\mathrm{T}}\boldsymbol{\alpha}\boldsymbol{\Phi}_{\mathbf{q}}\right)\ddot{\mathbf{q}}^{(i+1)} = \mathbf{P}\ddot{\mathbf{q}}^* - \boldsymbol{\Phi}_{\mathbf{q}}^{\mathrm{T}}\left[\boldsymbol{\kappa}^{(i+1)} + \varsigma\boldsymbol{\alpha}\left(\dot{\boldsymbol{\Phi}}_{\mathbf{q}}\dot{\mathbf{q}} + \dot{\boldsymbol{\Phi}}_t\right)\right] \tag{7a}$$

$$\boldsymbol{\kappa}^{(i+1)} = \boldsymbol{\kappa}^{(i)} + \varsigma\boldsymbol{\alpha}\ddot{\boldsymbol{\Phi}} \tag{7b}$$

where $\boldsymbol{\kappa}$ are the Lagrange multipliers associated to the projections of accelerations.

The projection equations (6) and (7) follow an iterative augmented Lagrangian scheme as in the case of the equations of motion (1). The update equations (6b) and (7b) are intended to make the Lagrange multipliers of the projections, $\boldsymbol{\sigma}$ and $\boldsymbol{\kappa}$, converge together with the fixed-point iterations (6a), (7a).

In [12], the following choices were proposed for $\mathbf{P}$ and ς:

1. The mass-orthogonal projections of Bayo and Ledesma [16]: $\mathbf{P} = \mathbf{M}$, $\varsigma = 1$.
2. The mass-stiffness-damping-orthogonal projections of Cuadrado et al. [17]: $\mathbf{P} = \mathbf{M} + \gamma h \mathbf{C} + \beta h^2 \mathbf{K}$, $\varsigma = \beta h^2$, where γ and β are scalar coefficients of the time-stepping integrator chosen.
3. The mass-stiffness-damping-Jacobian-orthogonal projections: $\mathbf{P} = \mathbf{M} + \gamma h \mathbf{C} + \beta h^2 \left[\boldsymbol{\Phi}_{\mathbf{qq}}^{\mathrm{T}} \left(\boldsymbol{\alpha}\boldsymbol{\Phi} + \boldsymbol{\lambda}^*\right) + \mathbf{K}\right]$, $\varsigma = \beta h^2$.

3. Forward sensitivity of the ALI3-P formulation

The problem is to obtain the sensitivity of the following objective function, defined in terms of the parameters, $\boldsymbol{\rho} \in \mathbb{R}^p$, the states and their derivatives $\mathbf{q}, \dot{\mathbf{q}}, \ddot{\mathbf{q}} \in \mathbb{R}^{n_c}$ and, maybe, the Lagrange multipliers of the dynamics $\boldsymbol{\lambda}^* \in \mathbb{R}^m$ and the Lagrange multipliers of the projections $\boldsymbol{\sigma}$ and $\boldsymbol{\kappa} \in \mathbb{R}^m$.

$$\psi = w\left(\mathbf{q}_F, \dot{\mathbf{q}}_F, \ddot{\mathbf{q}}_F, \boldsymbol{\lambda}_F^*, \boldsymbol{\sigma}_F, \boldsymbol{\kappa}_F, \boldsymbol{\rho}_F\right) + \int_{t_0}^{t_F} g\left(\mathbf{q}, \dot{\mathbf{q}}, \ddot{\mathbf{q}}, \boldsymbol{\lambda}^*, \boldsymbol{\sigma}, \boldsymbol{\kappa}, \boldsymbol{\rho}\right) \mathrm{d}t. \tag{8}$$

The sensitivity of such a cost function is expressed by the following gradient,

$$\begin{aligned} \nabla_{\boldsymbol{\rho}} \psi^{\mathrm{T}} = & \left(w_{\mathbf{q}} \mathbf{q}_{\boldsymbol{\rho}} + w_{\dot{\mathbf{q}}} \dot{\mathbf{q}}_{\boldsymbol{\rho}} + w_{\ddot{\mathbf{q}}} \ddot{\mathbf{q}}_{\boldsymbol{\rho}} + w_{\boldsymbol{\lambda}^*} \boldsymbol{\lambda}_{\boldsymbol{\rho}}^* + w_{\boldsymbol{\sigma}} \boldsymbol{\sigma}_{\boldsymbol{\rho}} + w_{\boldsymbol{\kappa}} \boldsymbol{\kappa}_{\boldsymbol{\rho}} + w_{\boldsymbol{\rho}}\right)_F + \\ & \int_{t_0}^{t_F} \left(g_{\mathbf{q}} \mathbf{q}_{\boldsymbol{\rho}} + g_{\dot{\mathbf{q}}} \dot{\mathbf{q}}_{\boldsymbol{\rho}} + g_{\ddot{\mathbf{q}}} \ddot{\mathbf{q}}_{\boldsymbol{\rho}} + g_{\boldsymbol{\lambda}^*} \boldsymbol{\lambda}_{\boldsymbol{\rho}}^* + g_{\boldsymbol{\sigma}} \boldsymbol{\sigma}_{\boldsymbol{\rho}} + g_{\boldsymbol{\kappa}} \boldsymbol{\kappa}_{\boldsymbol{\rho}} + g_{\boldsymbol{\rho}}\right) \mathrm{d}t. \end{aligned} \tag{9}$$

In Eq. (9) the derivatives of functions w and g are known, since the objective function has a known expression. On the contrary, the magnitudes $\mathbf{q}_{\boldsymbol{\rho}}$, $\dot{\mathbf{q}}_{\boldsymbol{\rho}}$, $\ddot{\mathbf{q}}_{\boldsymbol{\rho}} \in \mathbb{R}^{n_c \times p}$, $\boldsymbol{\lambda}_{\boldsymbol{\rho}}^*$, $\boldsymbol{\sigma}_{\boldsymbol{\rho}}$, and $\boldsymbol{\kappa}_{\boldsymbol{\rho}} \in \mathbb{R}^{m \times p}$ are the sensitivity matrices solution of a set of p DAE systems called the Tangent Linear Model (TLM) of the equations of motion plus p velocity sensitivity projections and p acceleration sensitivity projections.

The Tangent Linear Model (TLM) of the equations of motion can be obtained by differentiating (1) with respect to each one of the parameters:

$$\frac{\mathrm{d}\mathbf{M}}{\mathrm{d}\rho_k}\ddot{\mathbf{q}}^* + \mathbf{M}\frac{\mathrm{d}\ddot{\mathbf{q}}}{\mathrm{d}\rho_k} + \frac{\mathrm{d}\boldsymbol{\Phi}_{\mathbf{q}}^{\mathrm{T}}}{\mathrm{d}\rho_k}\left(\boldsymbol{\lambda}^* + \boldsymbol{\alpha}\boldsymbol{\Phi}\right) + \boldsymbol{\Phi}_{\mathbf{q}}^{\mathrm{T}}\left(\frac{\mathrm{d}\boldsymbol{\lambda}^*}{\mathrm{d}\rho_k} + \boldsymbol{\alpha}\frac{\mathrm{d}\boldsymbol{\Phi}}{\mathrm{d}\rho_k}\right) = \frac{\mathrm{d}\mathbf{Q}}{\mathrm{d}\rho_k}, \tag{10}$$

$$\frac{\mathrm{d}\boldsymbol{\lambda}^{*(i+1)}}{\mathrm{d}\rho_k} = \frac{\mathrm{d}\boldsymbol{\lambda}^{*(i)}}{\mathrm{d}\rho_k} + \boldsymbol{\alpha}\frac{\mathrm{d}\boldsymbol{\Phi}}{\mathrm{d}\rho_k}, \quad i > 0; k = 1, \ldots, p. \tag{11}$$

The sensitivity of the velocity projections is obtained differentiating Eq. (6a) with respect to the system parameters

$$\begin{aligned} &\left[\frac{\mathrm{d}\mathbf{P}}{\mathrm{d}\rho_k} + \varsigma\left(\frac{\mathrm{d}\boldsymbol{\Phi}_{\mathbf{q}}^{\mathrm{T}}}{\mathrm{d}\rho_k}\boldsymbol{\alpha}\boldsymbol{\Phi}_{\mathbf{q}} + \boldsymbol{\Phi}_{\mathbf{q}}^{\mathrm{T}}\boldsymbol{\alpha}\frac{\mathrm{d}\boldsymbol{\Phi}_{\mathbf{q}}}{\mathrm{d}\rho_k}\right)\right]\dot{\mathbf{q}} + \left(\mathbf{P} + \varsigma\boldsymbol{\Phi}_{\mathbf{q}}^{\mathrm{T}}\boldsymbol{\alpha}\boldsymbol{\Phi}_{\mathbf{q}}\right)\frac{\mathrm{d}\dot{\mathbf{q}}^{(i+1)}}{\mathrm{d}\rho_k} = \\ &\quad \frac{\mathrm{d}\mathbf{P}}{\mathrm{d}\rho_k}\dot{\mathbf{q}}^* + \mathbf{P}\frac{\mathrm{d}\dot{\mathbf{q}}^*}{\mathrm{d}\rho_k} - \frac{\mathrm{d}\boldsymbol{\Phi}_{\mathbf{q}}^{\mathrm{T}}}{\mathrm{d}\rho_k}\left(\boldsymbol{\sigma} + \varsigma\boldsymbol{\alpha}\boldsymbol{\Phi}_t\right) - \boldsymbol{\Phi}_{\mathbf{q}}^{\mathrm{T}}\left(\frac{\mathrm{d}\boldsymbol{\sigma}^{(i+1)}}{\mathrm{d}\rho_k} + \varsigma\boldsymbol{\alpha}\frac{\mathrm{d}\boldsymbol{\Phi}_t}{\mathrm{d}\rho_k}\right) \end{aligned} \tag{12a}$$

$$\frac{\mathrm{d}\boldsymbol{\sigma}^{(i+1)}}{\mathrm{d}\rho_k} = \frac{\mathrm{d}\boldsymbol{\sigma}^{(i)}}{\mathrm{d}\rho_k} + \varsigma\boldsymbol{\alpha}\frac{\mathrm{d}\dot{\boldsymbol{\Phi}}}{\mathrm{d}\rho_k} \tag{12b}$$

Similarly, the sensitivity of the acceleration projections,

$$\begin{aligned} &\left[\frac{\mathrm{d}\mathbf{P}}{\mathrm{d}\rho_k} + \varsigma\left(\frac{\mathrm{d}\boldsymbol{\Phi}_{\mathbf{q}}^{\mathrm{T}}}{\mathrm{d}\rho_k}\boldsymbol{\alpha}\boldsymbol{\Phi}_{\mathbf{q}} + \boldsymbol{\Phi}_{\mathbf{q}}^{\mathrm{T}}\boldsymbol{\alpha}\frac{\mathrm{d}\boldsymbol{\Phi}_{\mathbf{q}}}{\mathrm{d}\rho_k}\right)\right]\ddot{\mathbf{q}} + \left(\mathbf{P} + \varsigma\boldsymbol{\Phi}_{\mathbf{q}}^{\mathrm{T}}\boldsymbol{\alpha}\boldsymbol{\Phi}_{\mathbf{q}}\right)\frac{\mathrm{d}\ddot{\mathbf{q}}^{(i+1)}}{\mathrm{d}\rho_k} = \frac{\mathrm{d}\mathbf{P}}{\mathrm{d}\rho_k}\ddot{\mathbf{q}}^* + \mathbf{P}\frac{\mathrm{d}\ddot{\mathbf{q}}^*}{\mathrm{d}\rho_k} \\ &\quad -\frac{\mathrm{d}\boldsymbol{\Phi}_{\mathbf{q}}^{\mathrm{T}}}{\mathrm{d}\rho_k}\left[\boldsymbol{\kappa}^{(i+1)} + \varsigma\boldsymbol{\alpha}\left(\dot{\boldsymbol{\Phi}}_{\mathbf{q}}\dot{\mathbf{q}} + \dot{\boldsymbol{\Phi}}_t\right)\right] - \boldsymbol{\Phi}_{\mathbf{q}}^{\mathrm{T}}\left[\frac{\mathrm{d}\boldsymbol{\kappa}^{(k+1)}}{\mathrm{d}\rho_k} + \varsigma\boldsymbol{\alpha}\left(\frac{\mathrm{d}\dot{\boldsymbol{\Phi}}_{\mathbf{q}}\dot{\mathbf{q}}}{\mathrm{d}\rho_k} + \frac{\mathrm{d}\dot{\boldsymbol{\Phi}}_t}{\mathrm{d}\rho_k}\right)\right] \end{aligned} \tag{13a}$$

$$\frac{\mathrm{d}\boldsymbol{\kappa}^{(i+1)}}{\mathrm{d}\rho_k} = \frac{\mathrm{d}\boldsymbol{\kappa}^{(i)}}{\mathrm{d}\rho_k} + \varsigma\boldsymbol{\alpha}\frac{\mathrm{d}\ddot{\boldsymbol{\Phi}}}{\mathrm{d}\rho_k} \tag{13b}$$

Expanding the total derivatives in (10) and (11) and grouping them together in tensor-matrix notation leads to the following set of p DAEs:

$$\begin{aligned}\mathbf{M}\ddot{\mathbf{q}}^*_{\boldsymbol{\rho}} + \mathbf{C}\dot{\mathbf{q}}^*_{\boldsymbol{\rho}} + \left(\mathbf{M}_{\mathbf{q}}\ddot{\mathbf{q}}^* + \boldsymbol{\Phi}^{\mathrm{T}}_{\mathbf{qq}}\left(\boldsymbol{\lambda}^* + \boldsymbol{\alpha}\boldsymbol{\Phi}\right) + \boldsymbol{\Phi}^{\mathrm{T}}_{\mathbf{q}}\boldsymbol{\alpha}\boldsymbol{\Phi}_{\mathbf{q}} + \mathbf{K}\right)\mathbf{q}_{\boldsymbol{\rho}} + \boldsymbol{\Phi}^{\mathrm{T}}_{\mathbf{q}}\boldsymbol{\lambda}^*_{\boldsymbol{\rho}} = \\ \mathbf{Q}_{\boldsymbol{\rho}} - \mathbf{M}_{\boldsymbol{\rho}}\ddot{\mathbf{q}}^* - \boldsymbol{\Phi}^{\mathrm{T}}_{\mathbf{q}\boldsymbol{\rho}}\left(\boldsymbol{\lambda}^* + \boldsymbol{\alpha}\boldsymbol{\Phi}\right) - \boldsymbol{\Phi}^{\mathrm{T}}_{\mathbf{q}}\boldsymbol{\alpha}\boldsymbol{\Phi}_{\boldsymbol{\rho}}\end{aligned} \tag{14a}$$

$$\boldsymbol{\lambda}^{*(i+1)}_{\boldsymbol{\rho}} = \boldsymbol{\lambda}^{*(i)}_{\boldsymbol{\rho}} + \boldsymbol{\alpha}\left(\boldsymbol{\Phi}_{\mathbf{q}}\mathbf{q}_{\boldsymbol{\rho}} + \boldsymbol{\Phi}_{\boldsymbol{\rho}}\right) \tag{14b}$$

where the following terms are tensor-vector products: $\mathbf{M}_{\mathbf{q}}\ddot{\mathbf{q}} \equiv \mathbf{M}_{\mathbf{q}} \otimes \ddot{\mathbf{q}}$, $\boldsymbol{\Phi}^{\mathrm{T}}_{\mathbf{qq}}\left(\boldsymbol{\lambda}^* + \boldsymbol{\alpha}\boldsymbol{\Phi}\right) \equiv \boldsymbol{\Phi}^{\mathrm{T}}_{\mathbf{qq}} \otimes \left(\boldsymbol{\lambda}^* + \boldsymbol{\alpha}\boldsymbol{\Phi}\right)$, $\mathbf{M}_{\boldsymbol{\rho}}\ddot{\mathbf{q}} \equiv \mathbf{M}_{\boldsymbol{\rho}} \otimes \ddot{\mathbf{q}}$, $\boldsymbol{\Phi}^{\mathrm{T}}_{\mathbf{q}\boldsymbol{\rho}}\left(\boldsymbol{\lambda}^* + \boldsymbol{\alpha}\boldsymbol{\Phi}\right) \equiv \boldsymbol{\Phi}^{\mathrm{T}}_{\mathbf{q}\boldsymbol{\rho}} \otimes \left(\boldsymbol{\lambda}^* + \boldsymbol{\alpha}\boldsymbol{\Phi}\right)$. Using the same notation one obtains the set of projected velocity sensitivities from Eqs. (12)

$$\begin{aligned}\left(\mathbf{P} + \varsigma\boldsymbol{\Phi}^{\mathrm{T}}_{\mathbf{q}}\boldsymbol{\alpha}\boldsymbol{\Phi}_{\mathbf{q}}\right)\dot{\mathbf{q}}^{(i+1)}_{\boldsymbol{\rho}} = \mathbf{P}\dot{\mathbf{q}}^*_{\boldsymbol{\rho}} + \frac{\mathrm{d}\mathbf{P}}{\mathrm{d}\boldsymbol{\rho}}\left(\dot{\mathbf{q}}^* - \dot{\mathbf{q}}^{(i)}\right) \\ -\boldsymbol{\Phi}^{\mathrm{T}}_{\mathbf{qq}}\left(\boldsymbol{\sigma} + \varsigma\boldsymbol{\alpha}\dot{\boldsymbol{\Phi}}\right)\mathbf{q}_{\boldsymbol{\rho}} - \boldsymbol{\Phi}^{\mathrm{T}}_{\mathbf{q}\boldsymbol{\rho}}\left(\boldsymbol{\sigma} + \varsigma\boldsymbol{\alpha}\dot{\boldsymbol{\Phi}}\right) - \boldsymbol{\Phi}^{\mathrm{T}}_{\mathbf{q}}\left(\boldsymbol{\sigma}^{(i+1)}_{\boldsymbol{\rho}} + \varsigma\boldsymbol{\alpha}\mathbf{b}^{\boldsymbol{\rho}}\right)\end{aligned} \tag{15a}$$

$$\boldsymbol{\sigma}^{(i+1)}_{\boldsymbol{\rho}} = \boldsymbol{\sigma}^{(i)}_{\boldsymbol{\rho}} + \varsigma\boldsymbol{\alpha}\frac{\mathrm{d}\dot{\boldsymbol{\Phi}}}{\mathrm{d}\boldsymbol{\rho}} \tag{15b}$$

and the projected accelerations sensitivities from Eqs. (13)

$$\begin{aligned}\left(\mathbf{P} + \varsigma\boldsymbol{\Phi}^{\mathrm{T}}_{\mathbf{q}}\boldsymbol{\alpha}\boldsymbol{\Phi}_{\mathbf{q}}\right)\ddot{\mathbf{q}}^{(i+1)}_{\boldsymbol{\rho}} = \mathbf{P}\ddot{\mathbf{q}}^*_{\boldsymbol{\rho}} + \frac{\mathrm{d}\mathbf{P}}{\mathrm{d}\boldsymbol{\rho}}\left(\ddot{\mathbf{q}}^* - \ddot{\mathbf{q}}^{(i)}\right) \\ -\boldsymbol{\Phi}^{\mathrm{T}}_{\mathbf{qq}}\left(\boldsymbol{\kappa} + \varsigma\boldsymbol{\alpha}\ddot{\boldsymbol{\Phi}}\right)\mathbf{q}_{\boldsymbol{\rho}} - \boldsymbol{\Phi}^{\mathrm{T}}_{\mathbf{q}\boldsymbol{\rho}}\left(\boldsymbol{\kappa} + \varsigma\boldsymbol{\alpha}\ddot{\boldsymbol{\Phi}}\right) - \boldsymbol{\Phi}^{\mathrm{T}}_{\mathbf{q}}\left(\boldsymbol{\kappa}^{(i+1)}_{\boldsymbol{\rho}} + \varsigma\boldsymbol{\alpha}\mathbf{c}^{\boldsymbol{\rho}}\right)\end{aligned} \tag{16a}$$

$$\boldsymbol{\kappa}^{(i+1)}_{\boldsymbol{\rho}} = \boldsymbol{\kappa}^{(i)}_{\boldsymbol{\rho}} + \varsigma\boldsymbol{\alpha}\frac{\mathrm{d}\ddot{\boldsymbol{\Phi}}}{\mathrm{d}\boldsymbol{\rho}} \tag{16b}$$

where

$$\frac{\mathrm{d}\dot{\boldsymbol{\Phi}}}{\mathrm{d}\boldsymbol{\rho}} = \boldsymbol{\Phi}_{\mathbf{q}}\dot{\mathbf{q}}_{\boldsymbol{\rho}} + \mathbf{b}^{\boldsymbol{\rho}} \tag{17}$$

$$\frac{\mathrm{d}\ddot{\boldsymbol{\Phi}}}{\mathrm{d}\boldsymbol{\rho}} = \boldsymbol{\Phi}_{\mathbf{q}}\ddot{\mathbf{q}}_{\boldsymbol{\rho}} + \mathbf{c}^{\boldsymbol{\rho}} \tag{18}$$

$$\mathbf{b}^{\boldsymbol{\rho}} = \left(\boldsymbol{\Phi}_{\mathbf{qq}}\dot{\mathbf{q}} + \boldsymbol{\Phi}_{t\mathbf{q}}\right)\mathbf{q}_{\boldsymbol{\rho}} + \boldsymbol{\Phi}_{\mathbf{q}\boldsymbol{\rho}}\dot{\mathbf{q}} + \boldsymbol{\Phi}_{t\boldsymbol{\rho}} \tag{19}$$

$$\mathbf{c}^{\boldsymbol{\rho}} = \left(\boldsymbol{\Phi}_{\mathbf{qq}}\dot{\mathbf{q}} + \dot{\boldsymbol{\Phi}}_{\mathbf{q}} + \boldsymbol{\Phi}_{t\mathbf{q}}\right)\dot{\mathbf{q}}_{\boldsymbol{\rho}} + \left(\boldsymbol{\Phi}_{\mathbf{qq}}\ddot{\mathbf{q}} + \left(\dot{\boldsymbol{\Phi}}_{\mathbf{q}}\right)_{\mathbf{q}}\dot{\mathbf{q}} + \left(\dot{\boldsymbol{\Phi}}_{t}\right)_{\mathbf{q}}\right)\mathbf{q}_{\boldsymbol{\rho}} + \boldsymbol{\Phi}_{\mathbf{q}\boldsymbol{\rho}}\ddot{\mathbf{q}} + \left(\dot{\boldsymbol{\Phi}}_{\mathbf{q}}\right)_{\boldsymbol{\rho}}\dot{\mathbf{q}} + \left(\dot{\boldsymbol{\Phi}}_{t}\right)_{\boldsymbol{\rho}} \tag{20}$$

Observe that the term $\mathrm{d}\mathbf{P}/\mathrm{d}\boldsymbol{\rho}$ depends on the selection of the projection matrix. For the numerical experiments reported in this paper, Bayo's mass-orthogonal projections were selected. Accordingly,

$$\frac{\mathrm{d}\mathbf{P}}{\mathrm{d}\boldsymbol{\rho}} = \mathbf{M}_{\mathbf{q}}\mathbf{q}_{\boldsymbol{\rho}} + \mathbf{M}_{\boldsymbol{\rho}} \tag{21}$$

3.1. Algorithm implementation

The TLM in Eqs. (14) features four sets of unknowns, namely $\mathbf{q}_{\boldsymbol{\rho}}$, $\dot{\mathbf{q}}^*_{\boldsymbol{\rho}}$, $\ddot{\mathbf{q}}^*_{\boldsymbol{\rho}}$, and $\boldsymbol{\lambda}^*_{\boldsymbol{\rho}}$. Eq. (14a) can be reduced to a linear system of equations with the sensitivities $\mathbf{q}_{\boldsymbol{\rho}}$ as only unknowns introducing in it the numerical integrator expressions. If the Newmark integration scheme is used, then

$$\dot{\mathbf{q}}^*_{\boldsymbol{\rho},n} = \frac{\gamma}{\beta h}\mathbf{q}_{\boldsymbol{\rho},n} - \hat{\dot{\mathbf{q}}}_{\boldsymbol{\rho},n-1}; \qquad \text{where } \hat{\dot{\mathbf{q}}}_{\boldsymbol{\rho},n-1} = \frac{\gamma}{\beta h}\mathbf{q}_{\boldsymbol{\rho},n-1} + \left(\frac{\gamma}{\beta} - 1\right)\dot{\mathbf{q}}_{\boldsymbol{\rho},n-1} + h\left(\frac{\gamma}{2\beta} - 1\right)\ddot{\mathbf{q}}_{\boldsymbol{\rho},n-1} \tag{22a}$$

$$\ddot{\mathbf{q}}^*_{\boldsymbol{\rho},n} = \frac{1}{\beta h^2}\mathbf{q}_{\boldsymbol{\rho},n} - \hat{\ddot{\mathbf{q}}}_{\boldsymbol{\rho},n-1}; \qquad \text{where } \hat{\ddot{\mathbf{q}}}_{\boldsymbol{\rho},n-1} = \frac{1}{\beta h^2}\mathbf{q}_{\boldsymbol{\rho},n-1} + \frac{1}{\beta h}\dot{\mathbf{q}}_{\boldsymbol{\rho},n-1} + \left(\frac{1}{2\beta} - 1\right)\ddot{\mathbf{q}}_{\boldsymbol{\rho},n-1} \tag{22b}$$

and Eq. (14a) becomes, at instant $t = t_n$,

$$\begin{aligned}\left(\frac{1}{\beta h^2}\mathbf{M} + \frac{\gamma}{\beta h}\mathbf{C} + \mathbf{M}_{\mathbf{q}}\ddot{\mathbf{q}}^* + \boldsymbol{\Phi}^{\mathrm{T}}_{\mathbf{qq}}\left(\boldsymbol{\lambda}^* + \boldsymbol{\alpha}\boldsymbol{\Phi}\right) + \boldsymbol{\Phi}^{\mathrm{T}}_{\mathbf{q}}\boldsymbol{\alpha}\boldsymbol{\Phi}_{\mathbf{q}} + \mathbf{K}\right)\mathbf{q}_{\boldsymbol{\rho}} = \\ \mathbf{Q}_{\boldsymbol{\rho}} - \mathbf{M}_{\boldsymbol{\rho}}\ddot{\mathbf{q}}^* - \boldsymbol{\Phi}^{\mathrm{T}}_{\mathbf{q}\boldsymbol{\rho}}\left(\boldsymbol{\lambda}^* + \boldsymbol{\alpha}\boldsymbol{\Phi}\right) - \boldsymbol{\Phi}^{\mathrm{T}}_{\mathbf{q}}\boldsymbol{\alpha}\boldsymbol{\Phi}_{\boldsymbol{\rho}} - \boldsymbol{\Phi}^{\mathrm{T}}_{\mathbf{q}}\boldsymbol{\lambda}^*_{\boldsymbol{\rho}} + \mathbf{M}\hat{\ddot{\mathbf{q}}}_{\boldsymbol{\rho},n-1} + \mathbf{C}\hat{\dot{\mathbf{q}}}_{\boldsymbol{\rho},n-1}\end{aligned} \tag{23}$$

Still, an iterative solution process is required to ensure the convergence of the sensitivities of the Lagrange multipliers, $\boldsymbol{\lambda}^*_{\boldsymbol{\rho}}$, which enter the right-hand side in Eq. (23). Accordingly, this equation must be solved together with the iterative update provided in Eq. (14b). Upon convergence, the values of the sensitivities $\mathbf{q}_{\boldsymbol{\rho},n}$ and $\boldsymbol{\lambda}^*_{\boldsymbol{\rho},n}$ are known, and the approximate values of the sensitivities of the velocities and accelerations, $\dot{\mathbf{q}}^*_{\boldsymbol{\rho},n}$ and $\ddot{\mathbf{q}}^*_{\boldsymbol{\rho},n}$ can be obtained from the integrator equations, (22). Finally, the sensitivities of the projected velocities and accelerations, $\dot{\mathbf{q}}_{\boldsymbol{\rho},n}$ and $\ddot{\mathbf{q}}_{\boldsymbol{\rho},n}$ are obtained from the solution of the iterative processes in Eqs. (15)–(20). During this stage the sensitivities of the Lagrange multipliers of the projections, $\boldsymbol{\sigma}_{\boldsymbol{\rho}}$ and $\boldsymbol{\kappa}_{\boldsymbol{\rho}}$, are evaluated as well.

4. Numerical example

The test case considered in this work is the five-bar mechanism shown in Figure 1. This system is made up of five homogeneous rods connected by revolute joints at points A, 1, 2, 3, and B, with masses $m_{A1} = m_{3B} = 1$ kg, $m_{12} = m_{23} = 1.5$ kg. Gravity acts along the negative direction of the vertical axis, $g = 9.81$ m/s^2. Two linear springs with constant stiffness $k_1 = k_2 = 100$ N/m connect fixed point B with articulations 1 and 2. As parameters to obtain the sensitivities, the natural lengths of the springs were chosen, $\boldsymbol{\rho}^{\mathrm{T}} = [L_{01}, L_{02}]$. The values of these parameters were set to $L_{01} = \sqrt{2^2+1^2}$ m and $L_{02} = \sqrt{2^2+0.5^2}$ m. The system is initially at rest in the configuration shown in Fig. 1.

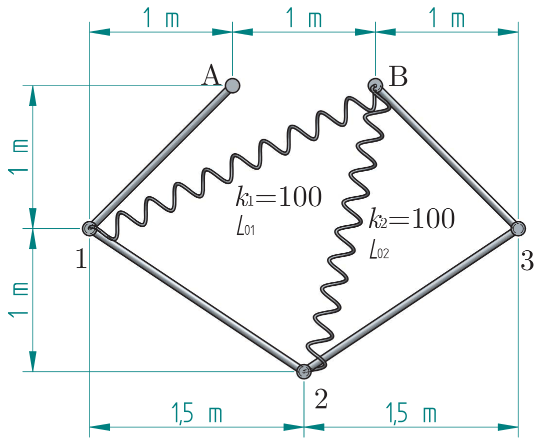

Figure 1: The five-bar mechanism

The sensitivities of this system are well known because they were previously obtained using several different formulations and approaches [18, 14]. The problem posed was the sensitivity analysis of the following objective function dependent on the solution of the equations of motion:

$$\psi = \int_{t_0}^{t_F} (\mathbf{r}_2 - \mathbf{r}_{20})^{\mathrm{T}} (\mathbf{r}_2 - \mathbf{r}_{20})\, \mathrm{d}t \tag{24}$$

where $\mathbf{r}_2$ is the global position of the point 2 and $\mathbf{r}_{20}$ is the initial position, at $t = t_0$, of the same point. Such an objective function was used in [14] to determine the natural lengths of the springs that make the system stay at rest in its initial configuration, by solving the unconstrained optimization problem $\boldsymbol{\rho} = \arg \min\limits_{\boldsymbol{\rho}} \psi$, nevertheless only sensitivities are of interest for this work.

The penalty formulation described in [14] was used as reference to validate the results obtained with the ALI3-P method described in Sections 2 and 3. A 5-s long numerical integration of the dynamics was carried out with the trapezoidal rule in Eqs. (2) and an integration step-size $h = 10^{-2}$ s.

Figure 2 shows the x- and y-components of the velocity of point 2 obtained with the penalty and the ALI3-P formulations. The mechanical energy of the system and its components, i.e., kinetic, gravitatory potential, and elastic potential, are shown in Fig. 3. The system is only subjected to the action of conservative forces and, as expected, the total mechanical energy remains constant. These results matched those obtained with other formulations, like the matrix R formulation and the index-1 DAE formulation, reported in [18] and [14].

After the integration of the equations of motion, the system sensitivities were evaluated as well using both the penalty and the ALI3-P formulations. The system sensitivities were integrated with the trapezoidal rule expressions for sensitivities in Eqs. (22) in the first case, and with the algorithm in Section 3.1 in the latter. Figs. 4–6 show the time-history

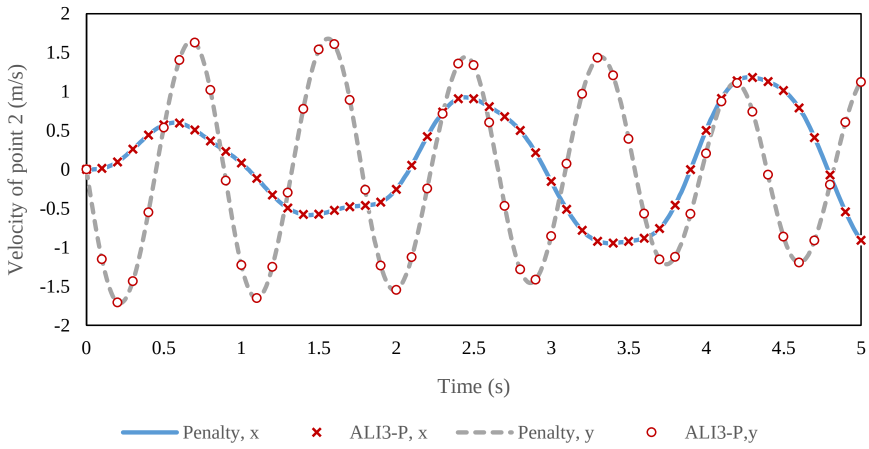

Figure 2: Velocities of point 2 obtained with the penalty and the ALI3-P formulations

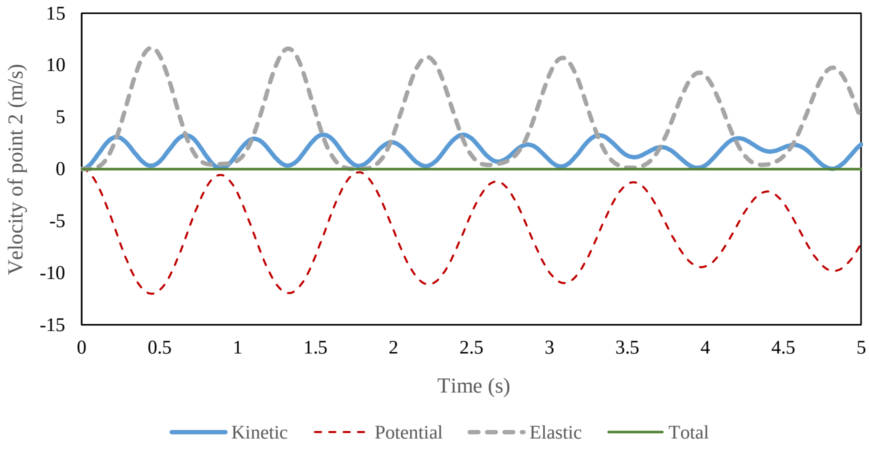

Figure 3: Components of the mechanical energy of the five-bar linkage. Both solution methods yielded similar results

of the sensitivities of the x-coordinate of point 2 at the configuration, velocity, and acceleration levels, with respect to the system parameters. The gradient obtained upon completion of the integration of the sensitivities at time $t_F = 5$ s with the ALI3-P method was $\nabla_{\boldsymbol{\rho}} \psi = \left[\ \mathrm{d}\psi/\mathrm{d}L_{01} \quad \mathrm{d}\psi/\mathrm{d}L_{02}\ \right] = \left[\ -4.2294 \quad 3.2114\ \right]$. The value obtained with the penalty formulation was $\nabla_{\boldsymbol{\rho}} \psi = \left[\ -4.2293 \quad 3.2112\ \right]$. These results are in the range reported in [14].

Given the fact that the system under study is subjected only to holonomic constraints, the contribution of the velocity and acceleration projections in Eqs. (15) and (16) to the sensitivity analysis is relatively small. In systems with nonholonomic constraints, however, the sensitivity of the projections could not be neglected, as these constraints are not enforced by the Newton-Raphson iteration in Eq. (4), but only by the velocity and acceleration projections in Eqs. (6a) and (7a). The contribution could also be relevant in systems with rheonomic constraints.

5. Conclusions

The present paper reports the sensitivity equations that correspond to the index-3 augmented Lagrangian formulation with velocity and acceleration projections, for multibody systems with holonomic constraints. The sensitivity equations were formulated as a Tangent Linear Model (TLM) for the Newton-Raphson iterative solution of the dynamics at the configuration level, plus two additional systems of equations for the velocity and acceleration projections. The algorithm equations can be combined with the numerical integration formulas to deliver the sensitivities of the system generalized coordinates as the solution of a system of nonlinear equations; the sensitivities of the generalized velocities and accelerations are obtained from the solution of the systems of nonlinear equations that result from the differentiation of the projections equations with respect to the system parameters.

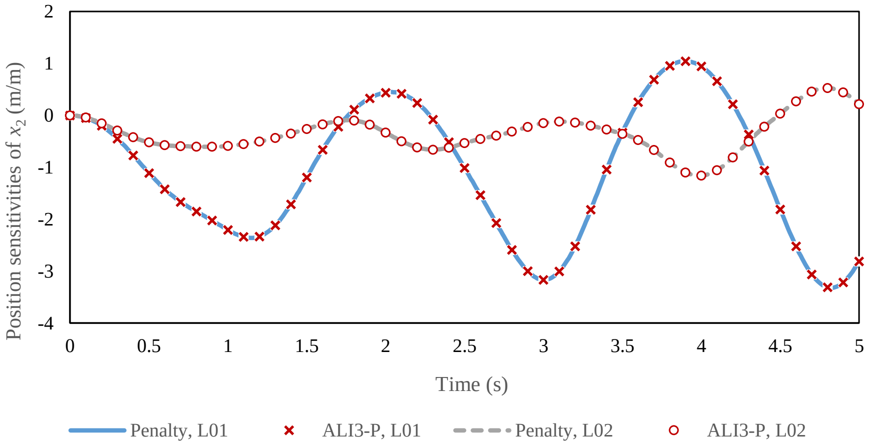

Figure 4: Sensitivities of the x-coordinate of point 2 with respect to the system parameters, evaluated with the penalty and the ALI3-P formulations

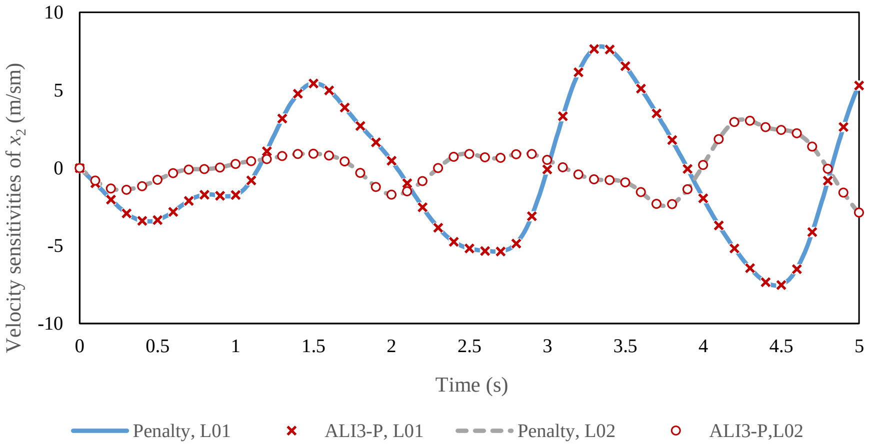

Figure 5: Sensitivities of the x-component of the velocity of point 2 with respect to the system parameters, evaluated with the penalty and the ALI3-P formulations

The proposed method was validated with the sensitivity analysis of a five-bar linkage with linear springs, which had been previously used in the literature as test problem for other sensitivity formulations. The results were compared to existing values in the literature to show that the sensitivity analysis of the example delivered correct results.

Acknowledgments

The support of the Spanish Ministry of Economy and Competitiveness (MINECO) under project DPI2016-81005-P and the post-doctoral research contract Juan de la Cierva No. JCI-2012-12376 is greatly acknowledged.

References

[1] C. O. Chang, P. E. Nikravesh. Optimal design of mechanical systems with constraint violation stabilization method. Journal of Mechanisms, Transmissions and Automation in Design, 107(4):493–498, 1985. doi: 10.1115/1.3260751.

[2] E. Haug. Computer aided optimal design: structural and mechanical systems, chapter Design sensitivity analysis of dynamic systems. Number 27 in NATO ASI series. Series F, Computer and systems sciences. Springer-Verlag, 1987.

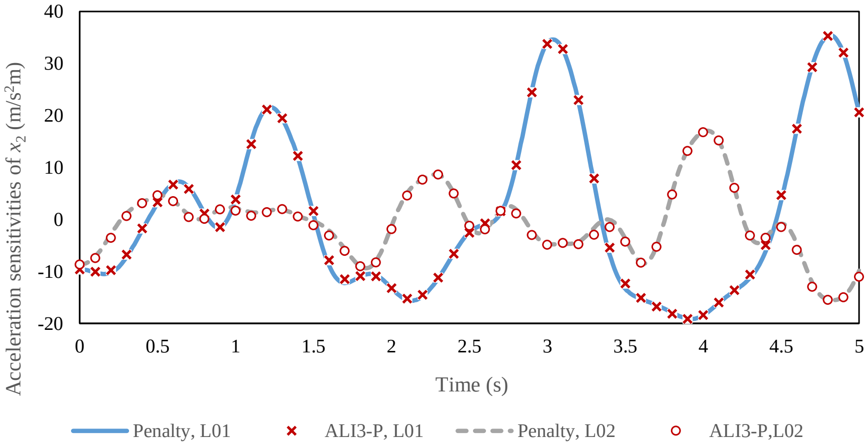

Figure 6: Sensitivities of the x-component of the acceleration of point 2 with respect to the system parameters, evaluated with the penalty and the ALI3-P formulations

[3] D. Bestle, J. Seybold. Sensitivity analysis of constrained multibody systems. Archive of Applied Mechanics, 62:181–190, 1992. doi:10.1007/BF00787958.

[4] D. Bestle, P. Eberhard. Analyzing and optimizing multibody systems. Mechanics of Structures and Machines, 20(1):67–92, 1992. doi:10.1080/08905459208905161.

[5] J. Pagalday, A. Avello. Optimization of multibody dynamics using object oriented programming and a mixed numerical-symbolic penalty formulation. Mechanism and Machine Theory, 32(2):161–174, 1997. doi: 10.1016/S0094-114X(96)00037-7.

[6] J. Dias, M. Pereira. Sensitivity analysis of rigid-flexible multibody systems. Multibody System Dynamics, 1:303–322, 1997. doi:10.1023/A:1009790202712.

[7] A. Schaffer. Stability of the adjoint differential-algebraic equation of the index-3 multibody system equation of motion. SIAM Journal on Scientific Computing, 26(4):1432–1448, 2005. doi:10.1137/030601983.

[8] A. Schaffer. Stabilized index-1 differential-algebraic formulations for sensitivity analysis of multi-body dynamics. Proceedings of the Institution of Mechanical Engineers Part K- Journal of Multi-Body Dynamics, 220(3):141–156, 2006. doi:10.1243/1464419JMBD62.

[9] J. Cuadrado, R. Gutierrez, M. Naya, P. Morer. A comparison in terms of accuracy and efficiency between a mbs dynamic formulation with stress analysis and a non-linear fea code. International Journal for Numerical Methods in Engineering, 51(9):1033–1052, 2001.

[10] D. Dopico, A. Luaces, M. González, J. Cuadrado. Dealing with multiple contacts in a human-in-the-loop application. Multibody System Dynamics, 25(2):167–183, 2011. doi:10.1007/s11044-010-9230-y.

[11] R. Pastorino, E. Sanjurjo, A. Luaces, M. A. Naya, W. Desmet, J. Cuadrado. Validation of a real-time multibody model for an X-by-wire vehicle prototype through field testing. Journal of Computational and Nonlinear Dynamics, 10(3):031006, 2015. doi:10.1115/1.4028030.

[12] D. Dopico, F. González, J. Cuadrado, J. Kövecses. Determination of holonomic and nonholonomic constraint reactions in an index-3 augmented Lagrangian formulation with velocity and acceleration projections. Journal of Computational and Nonlinear Dynamics, 9(4):041006–041006, 2014. doi:10.1115/1.4027671.

[13] F. González, D. Dopico, R. Pastorino, J. Cuadrado. Behaviour of augmented Lagrangian and Hamiltonian methods for multibody dynamics in the proximity of singular configurations. Nonlinear Dynamics, 85(3):1491–1508, 2016. doi:10.1007/s11071-016-2774-5.

[14] D. Dopico, A. Sandu, C. Sandu, Y. Zhu. Sensitivity Analysis of Multibody Dynamic Systems Modeled by ODEs and DAEs., chapter 1, 1–32. Multibody Dynamics - Computational Methods and Applications. Springer, 2014. doi:10.1007/978-3-319-07260-9.

[15] N. M. Newmark. A method of computation for structural dynamics. Journal of the Engineering Mechanics Division, ASCE, 85(EM3):67–94, 1959.

[16] E. Bayo, R. Ledesma. Augmented Lagrangian and mass-orthogonal projection methods for constrained multibody dynamics. Nonlinear Dynamics, 9(1-2):113–130, 1996.

[17] J. Cuadrado, J. Cardenal, P. Morer, E. Bayo. Intelligent simulation of multibody dynamics: Space-state and descriptor methods in sequential and parallel computing environments. Multibody System Dynamics, 4(1):55–73, 2000.

[18] D. Dopico, Y. Zhu, A. Sandu, C. Sandu. Direct and adjoint sensitivity analysis of ordinary differential equation multibody formulations. Journal of Computational and Nonlinear Dynamics, 10(1):1–8, 2014. doi: 10.1115/1.4026492.